B_1 Effects when Imaging Near Metal Implants at 3T

K. M. Koch[1], K. F. King[1], and G. C. McKinnon[1]
[1]Applied Science Laboratory, GE Healthcare, Waukesha, WI, United States

Introduction: The MAVRIC and SEMAC techniques enable low susceptibility-artifact imaging near metal implants using conventional spin-echo techniques [1,2]. Previous demonstrations of these techniques have been performed at 1.5T. Extending the techniques to 3T is easily feasible from a susceptibility artifact mitigation standpoint. This is due to the fact that both techniques restrict off-resonance effects to the applied RF bandwidths – which can be kept the same at 1.5T and 3T. However, it has previously been demonstrated that B_1 perturbations near metal implants become more prominent at 3T [3]. Here, we further explore this effect on MAVRIC images near a total hip replacement at 3T.

Theory: Perturbations to the transmitted B_1 magnetic field vary by implant geometries and the wavelength of applied radiation. Here, we consider the case of a metallic rod of length L oriented coaxial with B_0. When a homogeneous B_1 field of frequency ω is applied to a metallic rod, an electric potential

$$V = \frac{i\omega}{2}\int_L (\vec{r}\times\vec{B}_1)\bullet d\vec{l} \approx i\omega r B_1 L/2 \qquad [1]$$

is induced across it's length. Eqn 1 is a crude approximation that assumes a reference frame rotating at frequency ω in a cylindrical coordinate system where r is the radial coordinate [4]. The current along the length of the rod, I(x), can modeled as a standing wave (which approximates a lossless interaction with the surrounding medium):

$$I(x) = \frac{V}{Z+R}\sin(\pi\, x/\lambda) = kr\omega LB_1 \sin(\pi\, x/\lambda). \qquad [2]$$

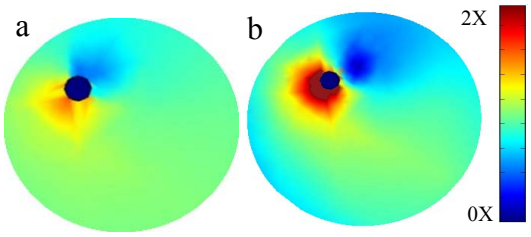

Figure 1: Axial maps of simulated flip-angle scaling for a 12cm (diameter 1cm) titanium rod collinear with B0 at (a) 1.5T and (b) 3T

where R is an effective resistance along the rod, Z is the effective impedance at the ends, and k is a proportionality constant. From this relationship we see that the induced current and it's contributing perturbation to the B_1 field is proportional to the frequency of applied radiation (ω), the axial position of the rod relative to the coil's center (r), and also has a standing wave effect depending on the wavelength of the applied radiation (λ). Based on this analysis, at rod lengths of $\lambda/2$, we expect to find a standing wave across the length of the rod. The wavelength of radiation in a perfect conductor is ~55cm at 64 MHz (1.5T) and ~30cm at 128 MHz (3.0T).

Simulations: Simulations of the B_1^+ field for a 12 cm titanium rod (radius 1 cm) were performed using the finite element solver provided by Comsol Multi-Physics™. The applied B_1^+ field was simulated from a 16 rung highpass birdcage body coil. A 30 cm long x 20 cm diameter water phantom was placed at the isocenter of the transmit coil and simulated to enclose the metal rod (relative permittivity of 60). The rod was axially offset from the center of the water phantom by 5 cm. Figure 1 presents the results of this simulation in the axial plane. The B_1^+ simulation results were used to construct relative flip-angle scaling maps around the rod. It is clear that the severity of the flip-angle modulation is dramatically increased at 3T in comparison to the simulation at 1.5T. Perturbations of the transmit field result in effective flip angles that are many times the intended angle in areas just below the rod (indicated by red in the displayed colormap). Simulations were also performed (not shown) with the rod was placed at the isocenter of the cylinder and at shorter rod lengths. As predicted by Eqn.[2], these factors significantly reduced the severity of the B_1^+ perturbations found near the rod. Compared to 64 MHz, the wavelength of radiation in the rod at 128 MHz (30 cm) is much closer to the standing wave mode λ=2L for the12 cm rod. Thus, the simulations qualitatively agree with the crude theoretical predictions outlined in Eqns [1-2].

Empirical Images: Empirical images are presented using the MAVRIC method [1]. Similar to images acquired at 1.5T, MAVRIC images at 3T will have residual frequency-encoded distortions on a sub-pixel level. In addition, marginal increases in signal loss may be found in the direct vicinity of implant interfaces, which is a result of increased implant-induced B_0 gradients.

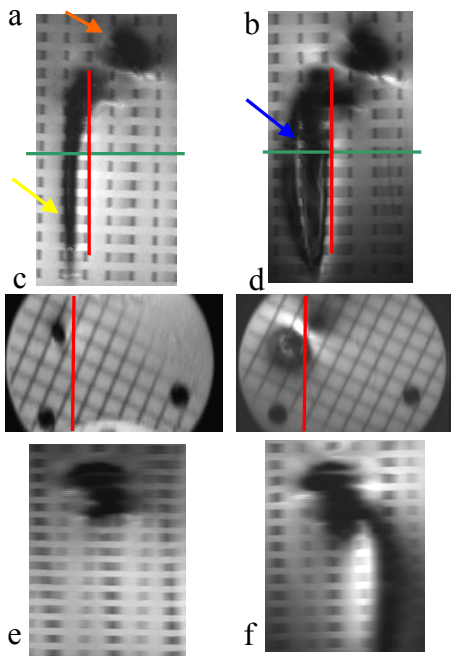

Figure 2: a) Coronal MAVRIC image of a total hip replacement at 1.5T and (b) 3T. Axial reformatted images at (c) 1.5T and (d) 3T -- reformat plane indicated by green line in (a,b). Coronal reformatted images at (e) 1.5T and (f) 3T – reformat indicated by red lines in (a,b,c,d).

Figure 1 (a,b) displays coronal MAVRIC images around a total hip replacement acquired at (a) 1.5T (refocusing flip angle 135°) and (b) 3T (refocusing flip angle 115°) with the shaft of the implant located 5 cm off of the transmit coil's isocenter. While the susceptibility artifact mitigation near the Cobalt-Chromium head (orange arrow, χ~1000 ppm) is similar between the two acquisitions, it is clear that the regions near the titanium shaft (yellow arrow, χ~180 ppm) are substantially impacted by the field increase. Figure 2 (c,d) provides axial reformats of the images at (c) 1.5T and (d) 3T (indicated by green lines on the coronal images), which coincides with the planes displayed in the simulations presented in Figure 1. As predicted by the simulations, the flip angle modulations induced at 1.5T have a relatively minor impact on the resulting image intensity, while the flip-angle modifications at 3T have a significant effect on the resulting image. Figure 2 (e,f) shows sagittal reformats (indicated by the red lines in the coronal and axial images) at (e)1.5T and (f) 3T.

The simulations presented in Figure 1 are for a simple cylindrical rod geometry. The titanium shaft in the hip implant is a much more complicated structure. However, it is clear that even this crude simulation is able to predict the general tenor of the B_1 perturbations induced by the titanium shaft and their impact on resulting FSE-based images. In particular, notice the line of signal parallel with the shaft indicated by the blue arrow in Figure 2 (b). This signal is available because the B_1 perturbations have resulted in an amplified flip angle corresponding to a full rotation of the magnetization. The signal is then lost as this flip angle reduces with distance from the implant. When the flip angle modulation is reduced to roughly 1.5x, then the signal is again recovered.

Conclusions We have shown that B_1 perturbations can substantially increase near metal implants as the wavelength of applied B_1 fields. While the susceptibility artifact reduction of the MAVRIC and SEMAC techniques will be similar between 1.5 and 3T, B_1 effects can become more prominent. In particular, long metallic structures collinear with B_0 will likely suffer significantly increased signal variations when imaged at 3T. Via finite element simulations, these effects have been isolated to perturbations of the transmitted B_1 field. This investigation suggests that B_1 effects are likely to be the dominant artifacts encountered when extending the MAVRIC and SEMAC methods to 3T, particularly near the shafts of total hip replacements.

[1] Koch et al,MRM,61,2009,381-390, [2] Lu et al,MRM,62,2009,66-76, [3] Graf et al, MRI, 23, 2005, 493-499, [4] Nitz et al, JMRI, 14, 2001, 105-114